



Design, synthesis and biological evaluation of some new 1,3,4-thiadiazine-thiourea derivatives as potential antitumor agents against non-small cell lung cancer cells

Fatma A.F. Ragab^a, Salah A. Abdel-Aziz^b, Marwa Kamel^c, Abdelsalam Mohamed A. Ouf^b, Heba Abdelrasheed Allam^{a,*}

^a Department of Pharmaceutical Chemistry, Faculty of Pharmacy, Cairo University, Kasr El-Aini Street, Cairo P.O. Box, 11562, Egypt

^b Department of Pharmaceutical Chemistry, Faculty of Pharmacy, Al-Azhar University, Assiut 71524, Egypt

^c Department of Cancer Biology, Unit of Pharmacology, National Cancer Institute, Cairo University, Egypt

ARTICLE INFO

Keywords:

1,3,4-thiadiazine
Thiourea
Non-small cell lung cancer
VEGFR2
B-RAF
MMP9

ABSTRACT

New 1,3,4-thiadiazine-thiourea derivatives have been synthesized. All the synthesized compounds were examined for *in vitro* cytotoxic activity against Non-Small Cell Lung Cancer (NSCLC) cell line A549, using MTT bioassay. Compounds **5d**, **5i**, **5j** showed the highest cytotoxic activity with IC₅₀ values of 0.27 ± 0.01 , 0.30 ± 0.02 , and $0.32 \pm 0.012 \mu\text{M}$ respectively with sorafenib as reference (IC₅₀ $3.85 \pm 0.27 \mu\text{M}$). These compounds were chosen for further investigations against various biological targets known to play roles in NSCLC specifically: vascular endothelial growth factor receptor 2 (VEGFR2), B-RAF and matrix metalloproteinase 9 (MMP9). Encouraging results were exhibited by the three compounds against the selected targets. Compound **5j** was specially promising as it exhibited inhibitory activity of VEGFR2 close to sorafenib (IC₅₀ $0.11 \pm 0.01 \mu\text{M}$), most potent B-RAF activity inhibition (IC₅₀ $0.178 \pm 0.004 \mu\text{M}$) and MMP9 inhibition (IC₅₀ $0.08 \pm 0.004 \mu\text{M}$). Moreover, cell cycle analysis of A549 cells treated with **5j** exhibited cell cycle arrest at G2-M phase and pro-apoptotic activity as indicated by Annexin V-FITC staining. Also, it reflected antinvasive and antimigration properties to A549 cells. Additionally, docking study of **5j** on VEGFR2, B-RAF and MMP9 revealed that it binds to the target enzymes in a similar way as the co-crystallized ligand. The three compounds exhibited significantly high selectivity to A549 cancer cells against the normal human fetal lung fibroblast cell line WI-38 with higher selectivity index compared to sorafenib (**5d** IC₅₀ $136.76 \pm 2.38 \mu\text{M}$, SI = 506.52; **5i** IC₅₀ $89.20 \pm 2.11 \mu\text{M}$, SI = 297.33; **5j** IC₅₀ $79.60 \pm 3.8 \mu\text{M}$, SI = 248.75; sorafenib IC₅₀ $30.32 \pm 2.41 \mu\text{M}$, SI = 7.88). In conclusion, compounds **5d**, **5i** and **5j**, specially **5j** are promising anticancer agents targeting important pathways in NSCLC and warrant further preclinical and clinical trials.

1. Introduction

According to global cancer statistics 2018, lung cancer is a commonly diagnosed cancer (11.6% of the total cases) and the principal cause of cancer death (18.4% of the total cancer deaths) [1]. It is categorized into two main histological groups: Small cell Lung cancer (SCLC) and Non-Small Cell Lung Cancer (NSCLC). NSCLC accounts for about 85% of cell lung cancers and are generally subcategorized into adenocarcinoma, squamous cell carcinoma, and large cell carcinoma [2]. One of the main challenges of several clinical trials of therapy of NSCLC is that blocking of one of the targeted pathways of signal transduction allows others to act as escape mechanisms for cancer cells. Therefore, a current strategy for cancer treatment involves the design of

multi-targeted anticancer agents [3]. Vascular endothelial growth factor (VEGF) represents a chief therapeutic target as it is a key angiogenic factor involved in tumor blood vessels formation [4]. Over expression of VEGF has been observed in a diversity of cancers including lung cancers and VEGF is a validated target for NSCLC [5]. Inhibition of VEGF or VEGF receptors (VEGFR) has been achieved either by using the monoclonal antibodies against VEGF such as bevacizumab [6] or by using tyrosine kinase inhibitors (TKIS) of VEGFR [7]. Sorafenib **I** acts as a multitargeting kinase inhibitor. It inhibits VEGFR2, VEGFR3, c-kit, PDGFR β and RAF and is indicated for hepatocellular carcinoma and advanced renal cell carcinoma. However, it has demonstrated only a moderate antitumor efficacy with numerous side effects in NSCLC, which greatly limits its clinical application [8].

* Corresponding author.

E-mail address: heba.abdelkalek@pharma.cu.edu.eg (H.A. Allam).

<https://doi.org/10.1016/j.bioorg.2019.103323>

Received 30 April 2019; Received in revised form 19 September 2019; Accepted 26 September 2019

Available online 26 September 2019

0045-2068/ © 2019 Elsevier Inc. All rights reserved.

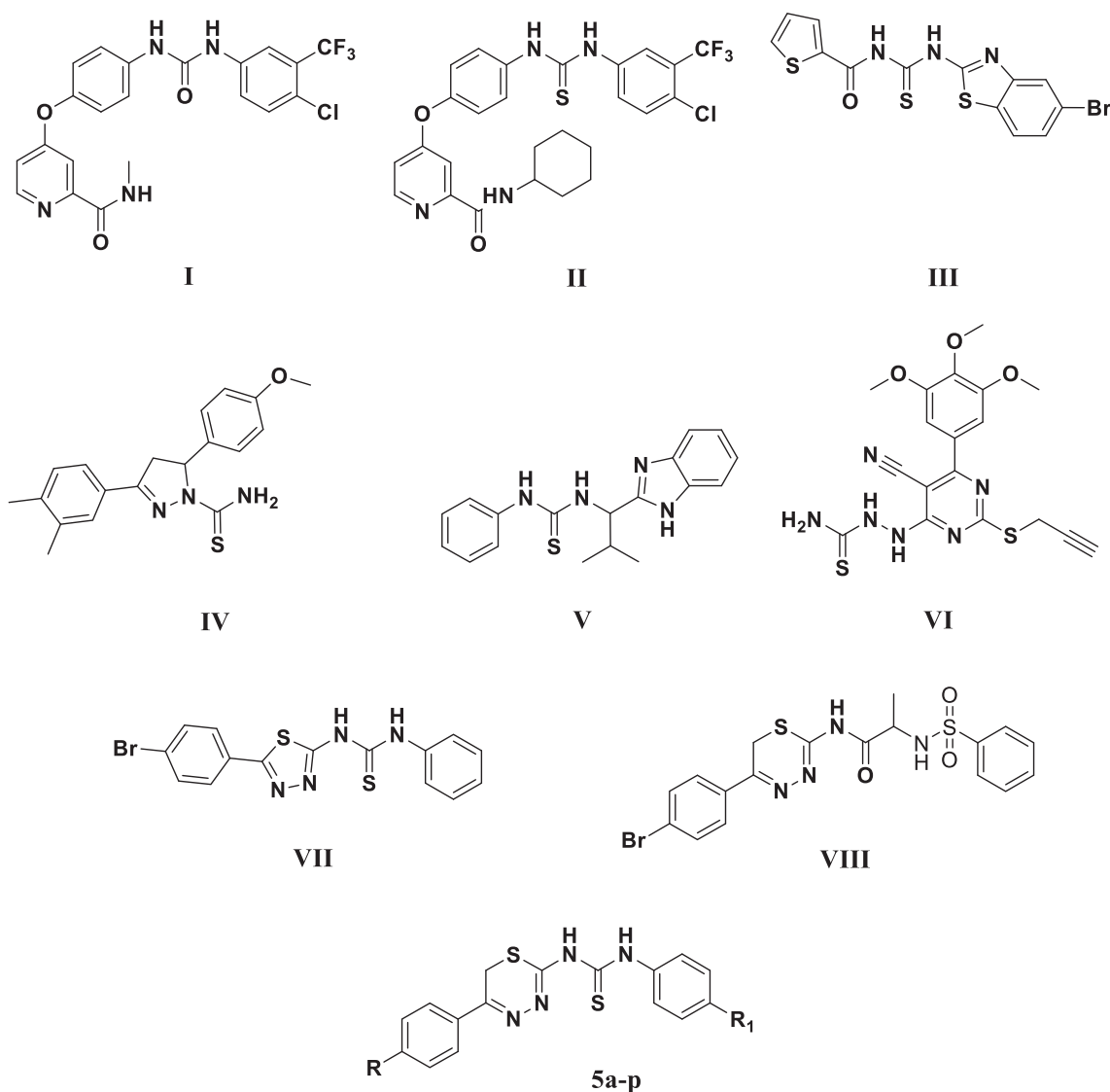


Fig. 1. Examples of anticancer compounds containing urea or thiourea moieties.

Several sorafenib thiourea derivatives **II** have been synthesized by substituting thiourea for urea moiety. Some of these derivatives demonstrated more potent inhibitory activities against cancer cells in addition to potent inhibitory activities against the phosphorylation of VEGFR [9–13].

On the other hand, several heterocyclic thiourea derivatives play important roles as anticancer agents against leukemia and solid tumors such as benzothiazole **III** [14,15], pyrazole **IV** [16], benzimidazole **V** [17], pyrimidine **VI** [18] and 1,3,4-thiadiazole **VII** [19]. 1,3,4-thiadiazole thiourea derivatives were found to have potent anticancer activity against A549 cell line [19]. However, the anticancer activity of 1,3,4-thiadiazines (ring expanded equivalent of 1,3,4-thiadiazole) thiourea hybrids have not widely been investigated although some reports mentioned that thiadiazine derivatives elicited inhibitory effect against various carcinoma cell lines. Moreover, some thiadiazine derivatives showed high inhibitory activities against different matrix metalloproteinases (MMPs) with high affinity to matrix metalloproteinase 9 (MMP9) **VIII** [20–23] (see Fig. 1). MMPs are enzymes which are overexpressed in different kinds of cancer comprising lung cancer and have critical roles in tumor invasion and metastasis [24].

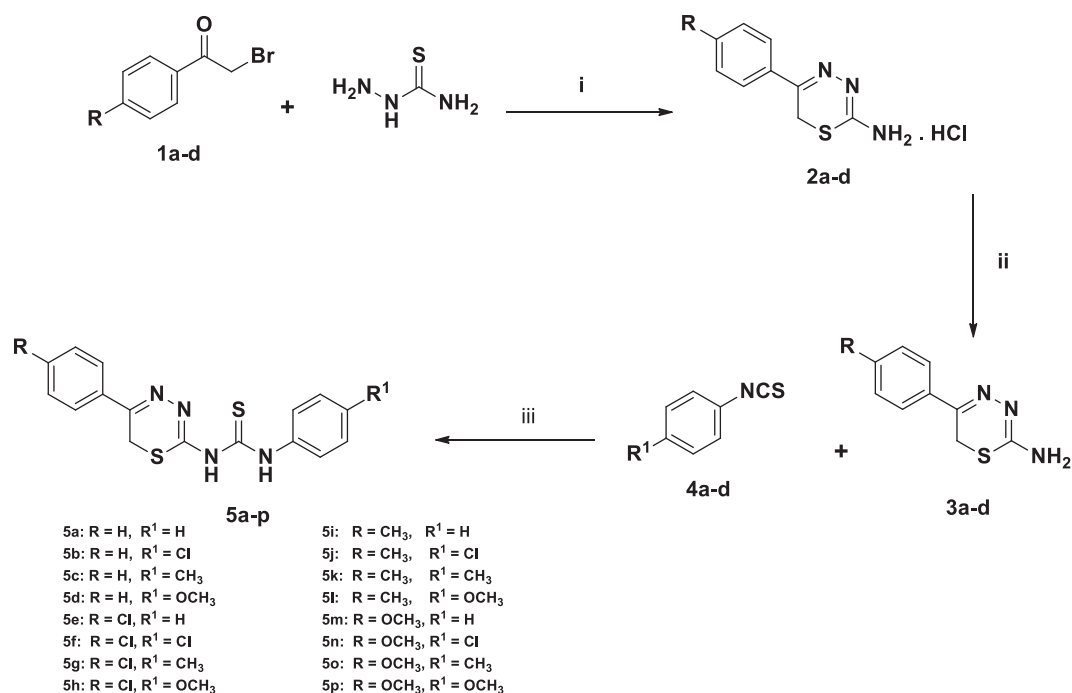
Consequently, the present investigation deals with the synthesis of a series of 1-substituted phenyl-3-(1,3,4-thiadiazinyl) thioureas **5a-p** to be evaluated for their cytotoxic activity against NSCLC (A549 cell line).

The most active derivatives were further evaluated for their VEGFR2 kinase activity as well as other targets including B-RAF and MMP9. Furthermore, cell cycle analysis, migration and invasion assays were performed for the most promising compound in order to gain additional insight about its mechanism of action. Also, molecular docking studies were performed to examine the binding interaction of the most promising compounds with VEGFR, B-RAF and MMP9 active sites.

2. Results and discussion

2.1. Chemistry

The general route for the synthesis of the target 1,3,4-thiadiazine-thiourea hybrids **5a-p** is represented in scheme I. Two general methods were available to prepare the synthon 2-Amino-5-aryl-6H-1,3,4-thiadiazine derivatives **3a-d**, firstly by reacting of substituted α -halo keto compounds with thiosemicarbazide in ethanol at 0 °C and the resulting linear intermediates were isolated and then ring closed by heating in ethanol/ H₂O/HBr mixture to afford the 5-substituted-6H-1,3,4-thiadiazine-2-Amine derivatives **3a-d** as their hydrochloride salts in good yields. In the second method the thiadiazine ring was constructed in one step from substituted α -halo keto compounds and thiosemicarbazide hydrochloride or hydrobromide in methanol [20].

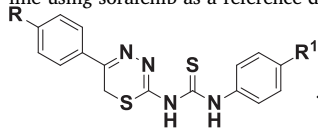


Reagents and conditions: (i) Conc HCl, EtOH, reflux; (ii) Aqueous ethanol, 7% solution of NH₃ (iii) Toluene, reflux.

Scheme 1. Synthesis of the target 1,3,4-thiadiazine thiourea derivatives. **Reagents and conditions:** (i) Conc HCl, EtOH, reflux; (ii) Aqueous ethanol, 7% solution of NH₃ (iii) Toluene, reflux.

Table 1

In vitro cytotoxic activity (IC₅₀) of compounds **5a-p** against A549 cancer cell line using sorafenib as a reference drug



Compound	R	R ¹	IC ₅₀ μM ± SE ^a
5a	H	H	1.48 ± 0.07*
5b	H	Cl	10.32 ± 0.51*
5c	H	CH ₃	1.39 ± 0.07*
5d	H	OCH ₃	0.27 ± 0.01*
5e	Cl	H	2.05 ± 0.10*
5f	Cl	Cl	4.47 ± 0.22
5g	Cl	CH ₃	2.50 ± 0.12*
5h	Cl	OCH ₃	3.23 ± 0.16
5i	CH ₃	H	0.30 ± 0.02*
5j	CH ₃	Cl	0.32 ± 0.02*
5k	CH ₃	CH ₃	1.70 ± 0.09*
5l	CH ₃	OCH ₃	0.97 ± 0.05*
5m	OCH ₃	H	2.77 ± 0.13*
5n	OCH ₃	Cl	3.55 ± 0.17
5o	OCH ₃	CH ₃	13.86 ± 0.69*
5p	OCH ₃	OCH ₃	21.99 ± 1.09*
Sorafenib			3.85 ± 0.27

^a IC₅₀ values are the means ± SE of three separate experiments.

* Statistically significant from sorafenib at p ≤ 0.05.

In the present work, compounds **3a-d** were prepared by a cyclocondensation reaction through stirring of phenacylbromide derivatives **1a-d** with thiosemicarbazide in ethanol at 0 °C for 3 h. Catalytic amount of hydrochloric acid was added to the stirred mixture then reflux for 1 h

to give the hydrochloride salt **2a-d**. Neutralization of **2a-d** by the addition of a 7% solution of NH₄OH with cooling gave the thiadiazine derivatives **3a-d** [25]. The thiourea derivatives **5a-p** were synthesized by refluxing of **3a-d** with various phenylisothiocyanates **4a-d** in toluene (Scheme 1).

The structure of compounds **5a-p** was confirmed by IR, ¹H NMR, ¹³C NMR, mass spectra and elemental analysis. The IR spectra exhibited two N–H stretching vibrations at 3286–3348, 3228–3273 cm⁻¹ and C=S stretching vibration at 1639–1720 cm⁻¹. ¹H NMR spectra displayed the presence of a singlet signal at δ 3.60–3.85 (CH₂ protons of the thiadiazine ring) and two singlet signals at δ 12.30–12.60, 10.50–10.70 (NH protons, D₂O exchangeable). Compounds **5c**, **5g**, **5k** and **5o** revealed a characteristic singlet signal at δ 2.27–2.40 (CH₃ protons of the *p*-tolyl part). Compounds **5i**, **5j**, **5k** and **5l** showed a characteristic singlet signal at δ 2.37 (CH₃ protons of the *p*-tolyl part attached to thiadiazine ring). Compounds **5d**, **5h**, **5l** and **5p** revealed the presence of a singlet signal at δ 3.74–3.80 (OCH₃ protons).

¹³C NMR spectra of compounds **5a**, **5b**, **5g**, **5h**, **5j**, **5k**, **5l**, **5n**, **5o** and **5p** revealed the presence of CS carbon at δ 183.93–184.36. Also, C2 of the thiadiazine ring gave a signal at δ 165.45–167.43. In addition, CH₂ of the thiadiazine ring gave a signal at δ 23.99–24.03. Moreover, compounds **5h**, **5l**, **5n**, **5o** and **5p** showed a characteristic signal at δ 55.69–55.80 assigned for OCH₃. Furthermore, compounds **5g**, **5j**, **5k** and **5l** were characterized by a signal at δ 20.98–21.42 related to CH₃.

2.2. Biological evaluation

2.2.1. MTT assay of the synthesized compounds

The newly synthesized compounds **5a-p** were screened for their cytotoxic activity against A549 cell line using MTT assay [26]. The cytotoxic activity was measured as the concentration that reduces the growth of the cancer cells by 50% represented as IC₅₀ μM. The IC₅₀ of compounds **5a-p** were presented in Table 1. Among the sixteen

Table 2
VEGFR2, B-RAF and MMP9 activity assay results of compounds **5d**, **5i** and **5j** using sorafenib as reference drug.

Compound	VEGFR2 IC ₅₀ μM ± SE ^a	B-RAF IC ₅₀ μM ± SE ^a	MMP9 IC ₅₀ μM ± SE ^a
5d	0.10 ± 0.01	0.66 ± 0.03*	3.015 ± 0.08*
5i	0.18 ± 0.01*	2.50 ± 0.07*	2.067 ± 0.04*
5j	0.11 ± 0.004	0.18 ± 0.004*	0.075 ± 0.01*
Sorafenib	0.11 ± 0.004	0.04 ± 0.002	0.02 ± 0.004

^a IC₅₀ values are the means ± SE of three separate experiments.

* Statistically significant from sorafenib at p ≤ 0.05.

compounds tested, twelve compounds showed more potent cytotoxic activity than sorafenib with IC₅₀ range 0.27 ± 0.013 to 3.55 ± 0.17 μM (sorafenib IC₅₀ = 3.85 ± 0.27 μM). Compounds **5d**, **5i** and **5j** were the most potent derivatives with IC₅₀ 0.27 ± 0.01, 0.30 ± 0.02, 0.32 ± 0.02 μM respectively. Variation of the aryl substituents attached to both the 5-position of thiadiazine nucleus and thiourea scaffold affected the cytotoxic activity. In general, it was observed that compounds **5i-l** substituted with a *p*-tolyl group at 5-position of thiadiazine nucleus exhibited more potent effect (IC₅₀ = 0.30 ± 0.02–1.70 ± 0.09 μM) than their analogues with 4-chlorophenyl group **5e-h** (IC₅₀ = 2.05 ± 0.10–4.47 ± 0.22 μM) or with 4-methoxyphenyl group **5m-p** (IC₅₀ = 2.77 ± 0.13–21.99 ± 1.09 μM) which gives an indication that the *p*-tolyl group at the thiadiazine nucleus is more beneficial for activity. In addition, derivatives with unsubstituted phenyl attached to thiadiazine nucleus showed promising activity except compound **5b**, while the most active compound was **5d** (IC₅₀ = 0.27 ± 0.01 μM).

2.2.2. VEGFR2 kinase activity assay of compounds **5d**, **5i** and **5j**

The most potent cytotoxic derivatives **5d**, **5i**, **5j** were further evaluated for their effects on VEGFR2 kinase activity. As indicated in Table 2, all the three compounds reduced the activity of the enzyme where compounds **5d** and **5j** exhibited VEGFR2 Kinase activity inhibition very close to sorafenib (**5d** IC₅₀ = 0.10 ± 0.01 μM; **5j** IC₅₀ = 0.11 ± 0.004 μM; sorafenib IC₅₀ = 0.11 ± 0.004 μM).

2.2.3. B-RAF kinase activity assay of compounds **5d**, **5i** and **5j**

RAF kinases (A-RAF, B-RAF and C-RAF (known also as RAF1) comprise important components of the RAS–RAF–MEK–ERK signaling cascade (ERK signaling) [27–29]. B-RAF mutations are present in many human tumors [30] such as melanomas (50%) [31], papillary thyroid cancers (45%) [32] and NSCLC (10%) [33]. Compounds **5d**, **5i**, **5j** were evaluated for their B-RAF inhibitory activities (Table 3). The most potent compound was **5j** (IC₅₀ = 0.18 ± 0.004 μM).

2.2.4. MMP9 inhibition screening assay of compounds **5d**, **5i** and **5j**

MMPs are family of zinc metalloproteinases which degrade the extracellular matrix and basement membranes. They play key roles in angiogenesis, inflammation, tumor development, cell proliferation and apoptosis [34]. Their activity is regulated by tissue inhibitors of

Table 3

In vitro cytotoxic activity (IC₅₀) of compounds **5d**, **5i** and **5j** against WI-38 cell line using sorafenib as a reference drug.

Compound	WI-38 IC ₅₀ μM ± SE ^a	Selectivity index (SI)
5d	136.76 ± 2.38*	506.52
5i	89.20 ± 2.11*	297.33
5j	79.6 ± 3.8*	248.75
Sorafenib	30.32 ± 2.41	7.88

^a IC₅₀ values are the means ± SE of three separate experiments.

* Statistically significant from sorafenib at p ≤ 0.05.

metalloproteinases [35]. Overexpression of MMP9 has been reported in NSCLC and is thus an interesting target for adjuvant anticancer therapy in NSCLC using specific inhibitors of MMP9 [36,37]. Thereby, in this study compounds **5d**, **5i** and **5j** were evaluated for their MMP9 inhibition response where they displayed promising inhibitory effect for the enzyme activities as represented in Table 3. Interestingly, compound **5j** exerted the most favorable response (IC₅₀ = 0.08 ± 0.01 μM).

2.2.5. Cell cycle analysis of compound **5j**

Based on the favorable effect of **5j** in inhibiting the activity of key enzymes involved in NSCLC, we were interested in the behavior of this compound on the cell cycle. Thus, influence of **5j** on A549 cells has been determined using flow cytometric analysis. Significant shifts in phases of the cell cycle resulted upon treatment of A549 cells with IC₅₀ concentration of **5j** (0.32 μM) for 24 h. The percentage of apoptotic cells at the pre-G phase was increased (12.64%) on exposure to **5j** compared to control (2.61%). Moreover, as shown in Fig. 2, there was a reduction in cell number at G0-G1 and S phases while there was an increased cell accumulation at G2-M phases which makes us speculate that compound **5j** inhibits the cell proliferation by means of cell cycle arrest at G2-M phase, thus prompting apoptotic cell death

2.2.6. Annexin V-FITC apoptosis assay

Additional assessment of the pro-apoptotic activity of compound **5j** was performed by Annexin V-FITC and propidium iodide double staining. Flow cytometric analysis of the differential binding of the cells to Annexin V-FITC and propidium iodide displayed a notable influence on the fraction of apoptotic cells. A549 cells treated with 0.32 μM of **5j** (IC₅₀) presented a rise in the percentage of Annexin V-FITC positive apoptotic cells (UR + LR) by 10.53% (6 folds) for **5j** (Fig. 3).

2.2.7. Cell invasion and migration assays

Since compound **5j** exhibited a promising effect on MMP9 activity, it was further assessed for its cell invasion and migration potentials. As shown in Fig. 4(A) **5j** decreased the invasion and migration of A549 by almost 2.5 and 2.4 folds respectively relative to control untreated cells. Similar effect was observed in Fig. 4(B). Collectively, these results demonstrate the promising effect of **5j** as an antimetastatic agent although it wasn't superior to sorafenib in this respect.

2.2.8. Cytotoxic activity against WI-38 human fetal lung fibroblast cell line

In order to assess the safety profile of compounds **5d**, **5i** and **5j**, MTT cytotoxicity assay was performed against normal human fetal lung fibroblast cell line WI-38 using sorafenib as a reference drug. The results infer that our selected compounds have significantly higher selectivity to A549 cancer cells compared to sorafenib (**5d** IC₅₀ 136.76 ± 2.38 μM, SI = 506.52; **5i** IC₅₀ 89.20 ± 2.11 μM, SI = 297.33; **5j** IC₅₀ 79.6 ± 3.8 μM, SI = 248.75; sorafenib IC₅₀ 30.32 ± 2.41 μM, SI = 7.88).

2.3. Docking study

The docking studies were performed to discover the possible binding mode of the most promising compound **5j** and its interaction with the main amino acids in the VEGFR2, B-RAF and MMP9 active sites. The **5j** was docked in the active sites of crystal structure of VEGFR2, B-RAF co-crystallized with sorafenib and MMP9 co-crystallized with reverse hydroxamate inhibitor. To ensure the accuracy of the docking protocol, validation was performed by redocking the co-crystallized ligand (sorafenib) into VEGFR2, B-RAF binding sites and reverse hydroxamate inhibitor into MMP9 active site. The docking poses were compared with the initial pose based on the binding mode and root mean square deviation (RMSD). The docking validation results displayed that, sorafenib docked nearly at the same position (RMSD = 0.691 Å) with energy score of −15.35 kcal/mol for VEGFR2

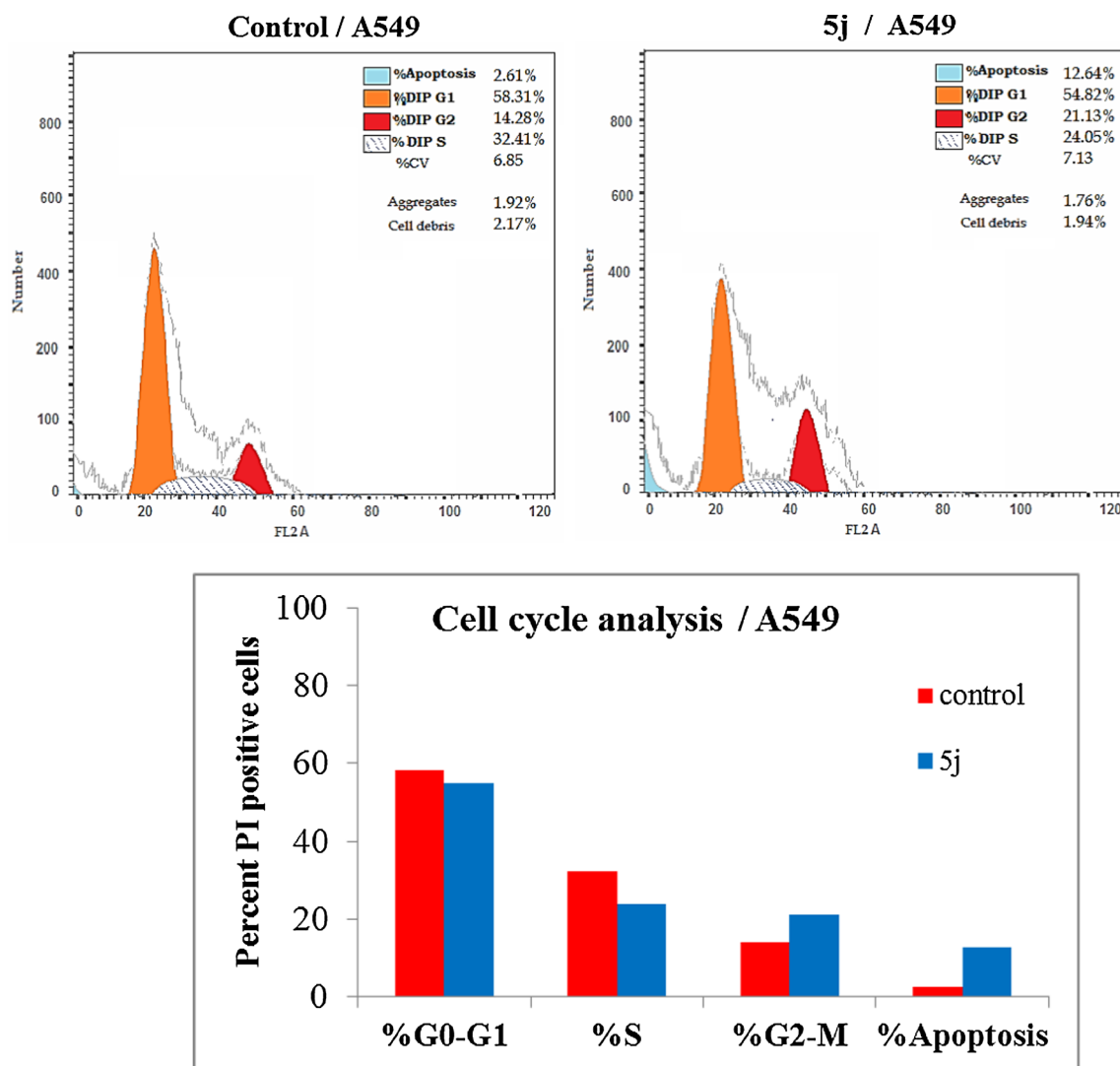


Fig. 2. Effect of 5j on DNA-ploidy flow cytometric analysis of A549 cells.

and B-RAF (RMSD = 0.6497 Å) with energy score of -14.75 kcal/mol while in the case of MMP9, RMSD was 0.9292 Å with energy score of -11.08 kcal/mol.

2.3.1. Docking results of compound 5j in VEGFR2

Compound 5j docked at the same position as sorafenib and displayed good interaction as indicated by hydrogen bonding with two of the key amino acids in the active site (Fig. 5). As a H-bond donor, the thiourea N–H attached to the thiadiazine ring interacts with Asp1046 (2.7 Å), while the anilino N–H interacts with the carboxylate side chain of Glu885 (2.6 Å) of the α C helix where the chlorophenyl moiety is fitted into the hydrophobic back pocket which is lined with the hydrophobic side chains of Ile888, Leu889, Val899, Cys1024 and Ile1025.

2.3.2. Docking results of compound 5j in B-RAF

Compound 5j docked at the same position as sorafenib and displayed good interaction as indicated by hydrogen bonding with two of the key amino acids in the active site (Fig. 6). As a H-bond donor, the thiourea N–H attached to the thiadiazine ring interacts with Asp594 (2.7 Å), while the anilino N–H interacts with the carboxylate side chain of Glu501 (2.5 Å) of the α C helix where the chlorophenyl moiety is fitted into the hydrophobic back pocket lined with the hydrophobic side chains of Leu514, Ile527, Val471 and Val482. Moreover, the phenyl group connected to the thiadiazine ring was included in π - π interaction

with the side chain of His574.

2.3.3. Docking results of compound 5j in MMP9

Compound 5j docked at the same position as reverse hydroxamate inhibitor and displayed good interaction as indicated by hydrogen bonding with essential glutamic acid residue (402) as well as the coordination bond of the catalytic zinc ion by His401, His405 and His411 is completed by both nitrogen atoms of the thiadiazine ring (Fig. 7).

3. Conclusion

In summary, new hybrids containing thiadiazine and thiourea fragments have been synthesized. All the synthesized compounds were investigated for their cytotoxic activity against A549 cell line. Compounds 5d, 5i and 5j showed the highest cytotoxic activities with IC_{50} range 0.27 ± 0.01 to 0.32 ± 0.02 μ M. These compounds have been selected to examine their effects on vital enzymes known to play roles in the pathogenesis of NSCLC namely VEGFR2, B-RAF and MMP9 using sorafenib as a reference drug. The three compounds exerted promising reduction to the enzyme activities and compound 5j was of special interest in this regards. 5j also exhibited cell cycle arrest at G2-M phase and pro-apoptotic, antinvasive and antimigration properties to A549 cells. Also, docking study of 5j revealed that it bound to the VEGFR2, B-RAF and MMP9 in a similar pattern as the co-crystallized

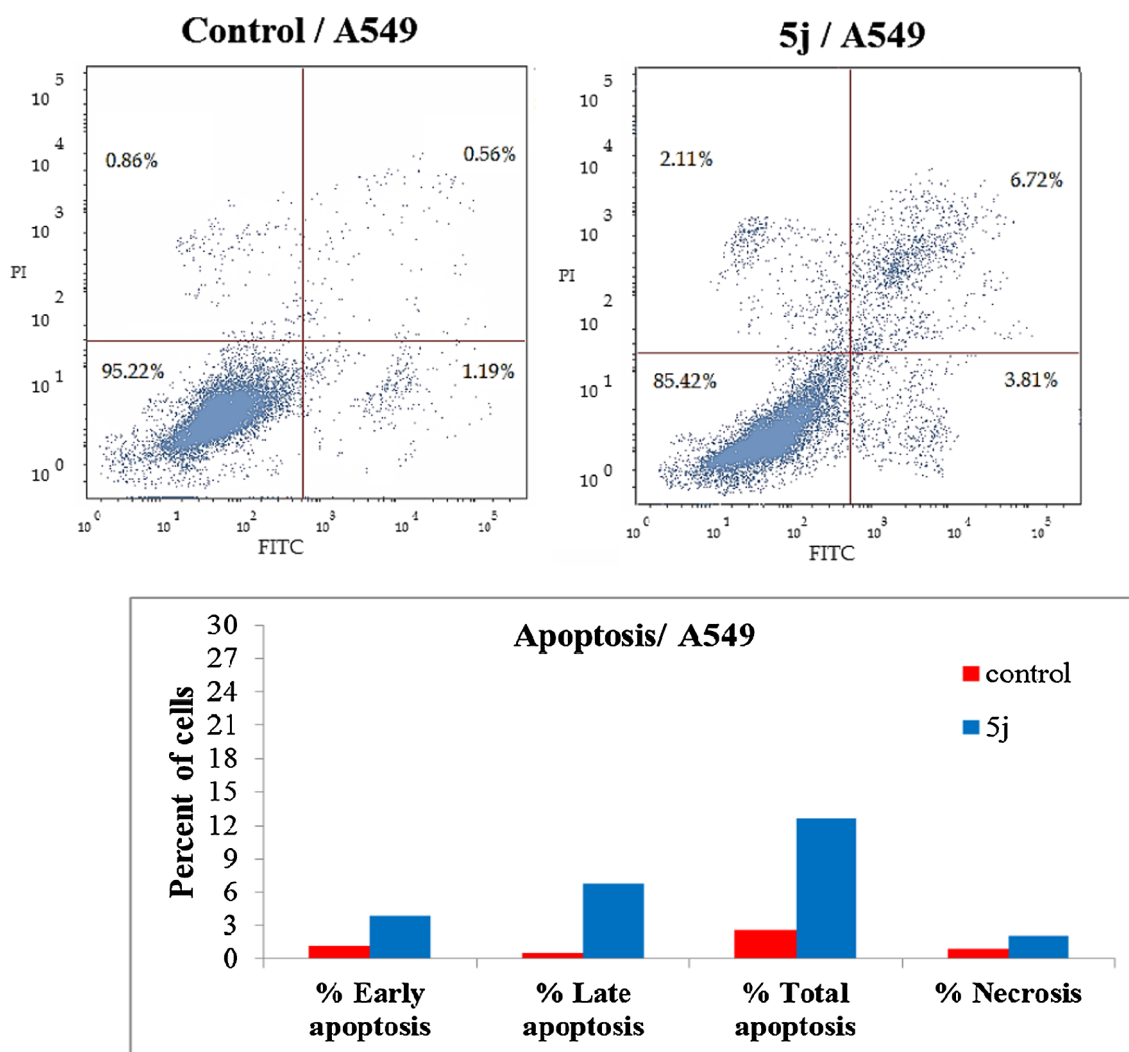


Fig. 3. Effect of 5j on the percentage of Annexin V-FITC-positive staining A549 cells.

ligand. The three compounds displayed safety against the normal lung fibroblast cell line WI-38 which indicates high selectivity against A549 cancer cells and potential safety profile to normal cells. Thus, based on this study we suggest that compounds **5d**, **5i** and **5j** are promising anticancer agents targeting key pathways implicated in NSCLC which qualifies them as suitable candidates for further preclinical and clinical trials.

4. Experimental

4.1. Chemistry

Unless otherwise mentioned, all chemicals were picked up from commercial suppliers and used without any further purification. Reactions were observed by TLC (Kieselgel 60 F254 precoated plates, E. Merck, Germany) and the spots were visualized by exposure to UV lamp at λ 254 nm. Determination of melting points was obtained by using of an electro thermal melting point apparatus (Stuart Scientific Co.). ^1H NMR and ^{13}C NMR spectra were determined in $\text{DMSO-}d_6$ and recorded on 400 MHz spectrophotometer for ^1H NMR and 100 MHz spectrophotometer for ^{13}C NMR (Bruker AG, Switzerland) at the Faculty of Pharmacy, Cairo University; Chemical shift (δ) values are expressed in parts per million (ppm) and coupling constants (J) in Hertz (Hz). Elemental microanalyses and mass spectrometry were carried out at the regional center for microbiology and biotechnology, Al-Azhar

University, Egypt. Infrared Spectra were performed on Shimadzu-FTIR spectrophotometer, Faculty of Pharmacy, Cairo University, Egypt and expressed in wave number (cm^{-1}), using potassium bromide discs.

Compounds **1a-d** and **3a-d** have been synthesized as reported [23,38–40].

4.1.1. Synthesis of compounds 5a-p

A mixture of 2-amino-5-aryl-6H-1,3,4-thiadiazine derivatives **3a-d** (2 mmol), and phenylisothiocyanate derivatives **4a-d** (2 mmol) was refluxed for 1 h in toluene. The reaction mixture was cooled to room temperature and the acquired yellow precipitate was filtered, washed with toluene then hexane, dried and crystallized using absolute ethanol.

4.1.1.1. 1-phenyl-3-(5-phenyl-6H-1,3,4-thiadiazin-2-yl) thiourea (5a). Yield, 89%; mp: 180–182 °C; IR (KBr) $\nu_{\text{max}}/\text{cm}^{-1}$ 3305, 3263, 2924, 1519. ^1H NMR δ 12.52 (s, 1H, NH, D_2O exchangeable), 10.69 (s, 1H, NH, D_2O exchangeable), 7.90–7.88 (m, 2H, Ar-H), 7.56–7.50 (m, 5H, Ar-H), 7.31 (t, $J = 7.5$ Hz, 2H, Ar-H), 7.08 (s, 1H, Ar-H), 3.87 (s, 2H, CH_2). ^{13}C NMR δ 184.36, 166.90, 149.39, 140.41, 134.55, 130.80, 129.32, 128.84, 127.03, 123.83, 122.09, 23.99. MS (m/z): 326 (M^+), 327 ($\text{M}^+ + 1$). Anal. Calcd for $\text{C}_{16}\text{H}_{14}\text{N}_4\text{S}_2$ (326.44): C, 58.87; H, 4.32; N, 17.16. Found: C, 59.12; H, 4.39; N, 17.34.

4.1.1.2. 1-(4-chlorophenyl)-3-(5-phenyl-6H-1,3,4-thiadiazin-2-yl)thiourea (5b). Yield, 90%; mp: 196–198 °C; IR (KBr) $\nu_{\text{max}}/\text{cm}^{-1}$ 3292, 3257,

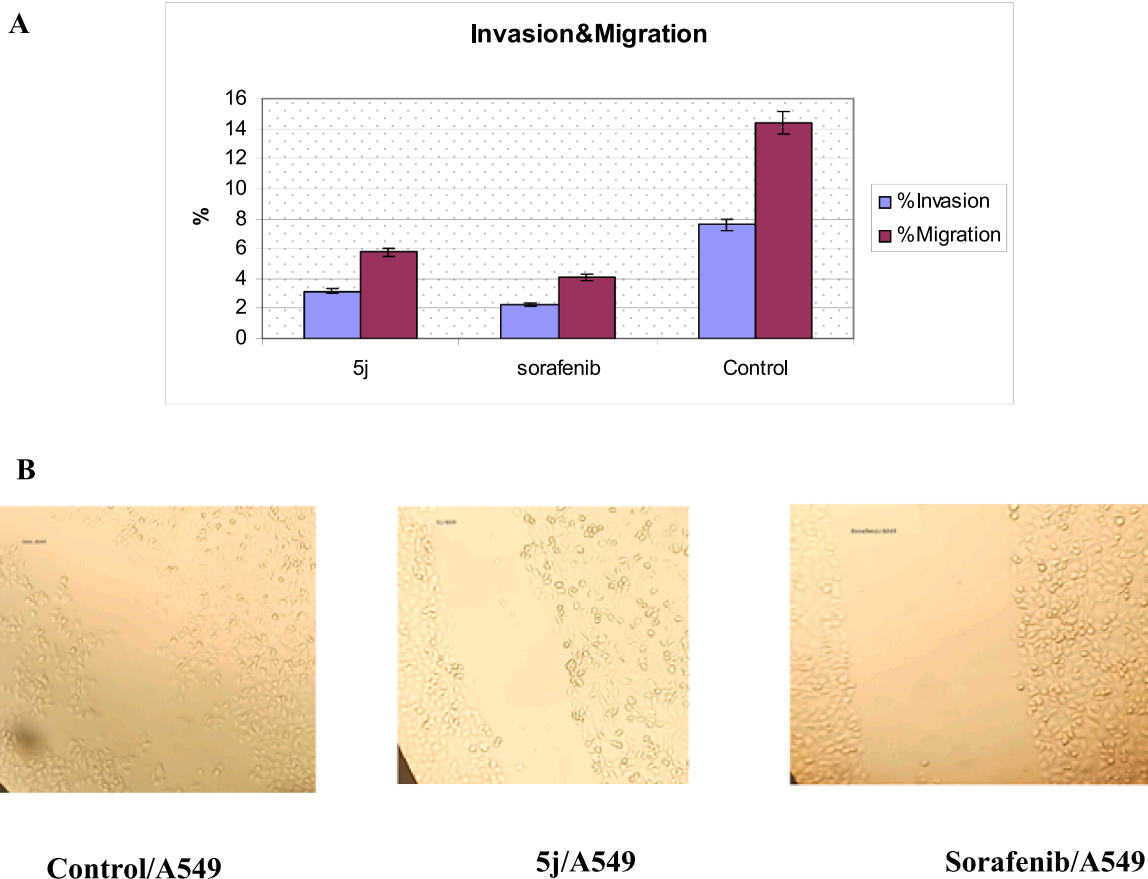


Fig. 4. Effect of 5j on invasion and migration of A549 cells as indicated by (A) Transwell membrane assay and (B) Wound healing assay.

2902, 1519. ^1H NMR δ 12.60 (s, 1H, NH, D_2O exchangeable), 10.76 (s, 1H, NH, D_2O exchangeable), 7.89–7.89 (m, 2H, Ar-H), 7.66–7.65 (m, 2H, Ar-H), 7.51–7.50 (m, 3H, Ar-H), 7.35 (d, $J = 7.9$ Hz, 2H, Ar-H), 3.88 (s, 2H, CH_2). ^{13}C NMR δ 184.26, 167.43, 149.47, 139.38, 134.47, 130.87, 129.33, 128.69, 127.49, 127.09, 123.51, 24.03. MS (m/z): 360 (M^+), 361 ($\text{M}^+ + 1$), 362 ($\text{M}^+ + 2$). Anal. Calcd. for $\text{C}_{16}\text{H}_{13}\text{ClN}_4\text{S}_2$ (360.88): C, 53.25; H, 3.63; N, 15.53. Found: C, 53.48; H, 3.72; N, 15.61.

4.1.1.3. 1-(5-phenyl-6H-1,3,4-thiadiazin-2-yl)-3-(p-tolyl)thiourea (5c). Yield, 87%; mp: 182–184 °C; IR (KBr) $\nu_{\text{max}}/\text{cm}^{-1}$ 3300, 3267, 2916, 1508. ^1H NMR δ 12.46 (s, 1H, NH, D_2O exchangeable), 10.62 (s,

1H, NH, D_2O exchangeable), 7.89–7.87 (m, 2H, Ar-H), 7.51–7.40 (m, 5H, Ar-H), 7.11–7.10 (m, 2H, Ar-H), 3.87 (s, 2H, CH_2), 2.27 (s, 3H, CH_3). MS (m/z): 340 (M^+), 341 ($\text{M}^+ + 1$). Anal. Calcd. for $\text{C}_{17}\text{H}_{16}\text{N}_4\text{S}_2$ (340.46): C, 59.97; H, 4.74; N, 16.46. Found: C, 59.62; H, 4.39; N, 16.64.

4.1.1.4. 1-(4-methoxyphenyl)-3-(5-phenyl-6H-1,3,4-thiadiazin-2-yl)thiourea (5d). Yield, 90%; mp: 176–178 °C; IR (KBr) $\nu_{\text{max}}/\text{cm}^{-1}$ 3309, 3248, 2924, 1506. ^1H NMR δ 12.40 (s, 1H, NH, D_2O exchangeable), 10.59 (s, 1H, NH, D_2O exchangeable), 7.91–7.87 (m, 3H, Ar-H), 7.60–7.49 (m, 3H, Ar-H), 7.41 (d, $J = 7.8$ Hz, 1H, Ar-H), 6.88–6.86 (m, 2H, Ar-H), 3.87 (s, 2H, CH_2), 3.74 (s, 3H, OCH_3). MS (m/z): 356

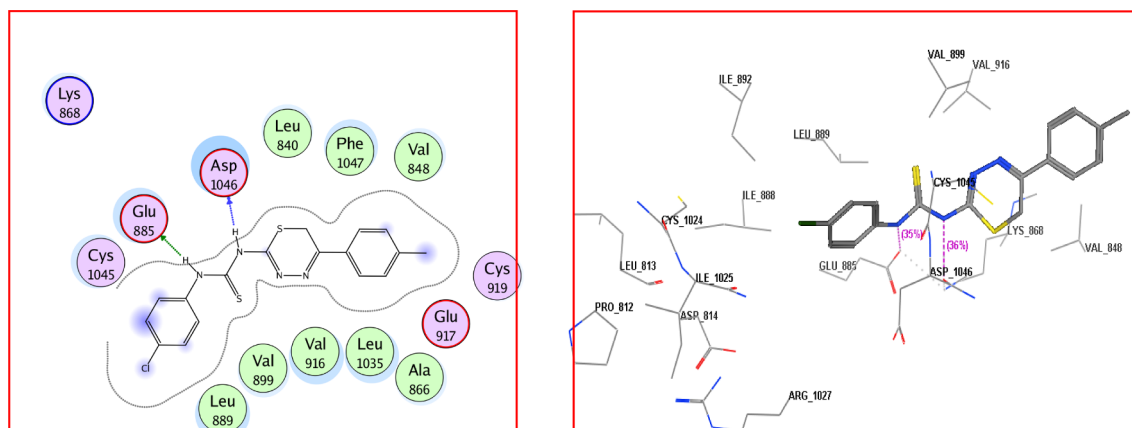


Fig. 5. The best docking pose of 5j in the active site of VEGFR-2 in 2D and 3D style.

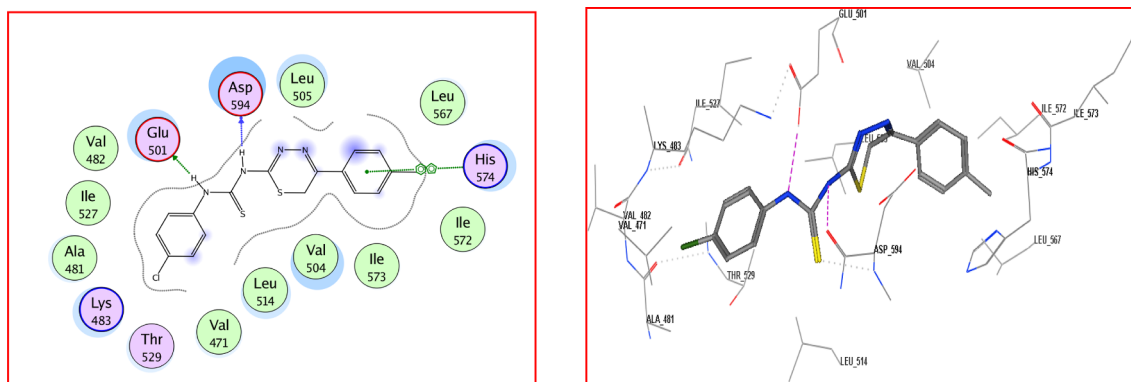


Fig. 6. The best docking pose of 5j in the active site of B-RAF in 2D and 3D style.

(M⁺), 357 (M⁺ + 1). Anal. Calcd. for C₁₇H₁₆N₄OS₂ (356.46): C, 57.28; H, 4.52; N, 15.72. Found: C, 57.49; H, 4.58; N, 15.68.

4.1.1.5. 1-(5-(4-chlorophenyl)-6H-1,3,4-thiadiazin-2-yl)-3-phenylthiourea (5e). Yield, 85%; mp: 179–180 °C; IR (KBr) $\nu_{\max}/\text{cm}^{-1}$ 3321, 3244, 2924, 1525. ¹H NMR δ 12.54 (s, 1H, NH, D₂O exchangeable), 10.72 (s, 1H, NH, D₂O exchangeable), 7.90 (d, *J* = 8.5 Hz, 2H, Ar-H), 7.57 (d, *J* = 8.6 Hz, 4H, Ar-H), 7.31 (t, *J* = 7.3 Hz, 2H, Ar-H), 7.08 (s, 1H, Ar-H), 3.87 (s, 2H, CH₂). MS (*m/z*): 360 (M⁺), 361 (M⁺ + 1), 362 (M⁺ + 2). Anal. Calcd. for C₁₆H₁₃ClN₄S₂ (360.88): C, 53.25; H, 3.63; N, 15.53. Found: C, 53.44; H, 3.60; N, 15.69.

4.1.1.6. 1-(4-chlorophenyl)-3-(5-(4-chlorophenyl)-6H-1,3,4-thiadiazin-2-yl) thiourea (5f). Yield, 78%; mp: 178–180 °C; IR (KBr) $\nu_{\max}/\text{cm}^{-1}$ 3348, 3228, 2900, 1512. ¹H NMR δ 12.62 (s, 1H, NH, D₂O exchangeable), 10.78 (s, 1H, NH, D₂O exchangeable), 7.91 (d, *J* = 8.6 Hz, 2H, Ar-H), 7.71–7.51 (m, 4H, Ar-H), 7.35 (d, *J* = 8.0 Hz, 2H, Ar-H), 3.87 (s, 2H, CH₂). MS (*m/z*): 394 (M⁺), 395 (M⁺ + 1), 396 (M⁺ + 2). Anal. Calcd. for C₁₆H₁₂Cl₂N₄S₂ (395.33): C, 48.61; H, 3.06; N, 14.17. Found: C, 48.50; H, 3.12; N, 14.05.

4.1.1.7. 1-(5-(4-chlorophenyl)-6H-1,3,4-thiadiazin-2-yl)-3-(*p*-tolyl) thiourea (5g). Yield, 83%; mp: 184–186 °C; IR (KBr) $\nu_{\max}/\text{cm}^{-1}$ 3286, 3267, 2920, 1516. ¹H NMR δ 12.48 (s, 1H, NH, D₂O exchangeable), 10.65 (s, 1H, NH, D₂O exchangeable), 7.90 (d, *J* = 8.5 Hz, 2H, Ar-H), 7.57 (d, *J* = 8.5 Hz, 3H, Ar-H), 7.39 (s, 1H, Ar-H), 7.16–7.11 (m, 2H, Ar-H), 3.86 (s, 2H, CH₂), 2.27 (s, 3H, CH₃). ¹³C NMR δ 184.20, 166.44, 148.15, 1380.34, 137.91, 135.48, 134.39, 133.44, 130.81, 129.37, 129.06, 128.75, 128.51, 126.22, 122.13, 23.78, 20.98. MS (*m/z*): 374

(M⁺), 375 (M⁺ + 1), 376 (M⁺ + 2). Anal. Calcd. for C₁₇H₁₅ClN₄S₂ (374.91): C, 54.46; H, 4.03; N, 14.94. Found: C, 54.67; H, 4.07; N, 15.08.

4.1.1.8. 1-(5-(4-chlorophenyl)-6H-1,3,4-thiadiazin-2-yl)-3-(4-methoxyphenyl) thiourea (5h). Yield, 80%; mp: 178–180 °C; IR (KBr) $\nu_{\max}/\text{cm}^{-1}$ 3317, 3251, 2927, 1504. ¹H NMR δ 12.44 (s, 1H, NH, D₂O exchangeable), 10.64 (s, 1H, NH, D₂O exchangeable), 7.89 (d, *J* = 8.3 Hz, 2H, Ar-H), 7.60–7.54 (m, 3H, Ar-H), 7.41 (d, *J* = 7.2 Hz, 1H, Ar-H), 6.96–6.87 (m, 2H, Ar-H), 3.94 (s, 2H, CH₂), 3.74 (s, 3H, OCH₃). ¹³C NMR δ 183.93, 166.24, 156.85, 156.09, 148.13, 147.82, 135.48, 133.65, 133.43, 129.35, 128.74, 125.10, 123.70, 114.07, 113.85, 55.69, 23.77. MS (*m/z*): 390 (M⁺). Anal. Calcd. for C₁₇H₁₅ClN₄OS₂ (390.90): C, 52.23; H, 3.87; N, 14.33. Found: C, 52.19; H, 3.90; N, 14.58.

4.1.1.9. 1-phenyl-3-(5-(*p*-tolyl)-6H-1,3,4-thiadiazin-2-yl)thiourea (5i). Yield, 89%; mp: 186–188 °C; IR (KBr) $\nu_{\max}/\text{cm}^{-1}$ 3304, 3253, 2916, 1519. ¹H NMR δ 12.48 (s, 1H, NH, D₂O exchangeable), 10.67 (s, 1H, NH, D₂O exchangeable), 7.79 (d, *J* = 8.0 Hz, 2H, Ar-H), 7.72–7.57 (m, 2H, Ar-H), 7.31 (d, *J* = 7.8 Hz, 4H, Ar-H), 7.08 (s, 1H, Ar-H), 3.84 (s, 2H, CH₂), 2.37 (s, 3H, CH₃). MS (*m/z*): 340 (M⁺), 341 (M⁺ + 1). Anal. Calcd. for C₁₇H₁₆N₄S₂ (340.46): C, 59.97; H, 4.74; N, 16.46. Found: C, 60.17; H, 4.76; N, 16.80.

4.1.1.10. 1-(4-chlorophenyl)-3-(5-(*p*-tolyl)-6H-1,3,4-thiadiazin-2-yl) thiourea (5j). Yield, 90%; mp: 190–192 °C; IR (KBr) $\nu_{\max}/\text{cm}^{-1}$ 3288, 3267, 2920, 1517. ¹H NMR δ 12.54 (s, 1H, NH, D₂O exchangeable), 10.73 (s, 1H, NH, D₂O exchangeable), 7.79 (d, *J* = 7.9 Hz, 2H, Ar-H),

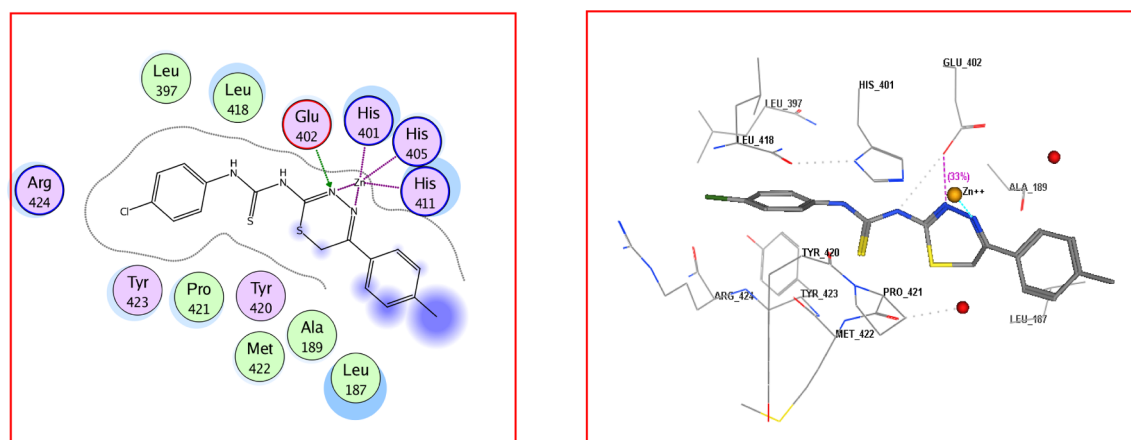


Fig. 7. The best docking pose of 5j in the active site of MMP9 in 2D and 3D style.

7.67–7.64 (m, 2H, Ar-H), 7.35–7.30 (m, 4H, Ar-H), 3.84 (s, 2H, CH₂), 2.37 (s, 3H, CH₃). ¹³C NMR δ 184.20, 167.72, 149.54, 140.81, 139.41, 131.67, 129.92, 128.67, 127.05, 123.57, 123.46, 23.97, 21.42. MS (*m/z*): 374 (M⁺), 375 (M⁺ + 1), 376 (M⁺ + 2). Anal. Calcd. for C₁₇H₁₅ClN₄S₂ (374.91): C, 54.46; H, 4.03; N, 14.94. Found: C, 54.62; H, 4.06; N, 15.12.

4.1.1.11. 1-(*p*-tolyl)-3-(5-(*p*-tolyl)-6H-1,3,4-thiadiazin-2-yl)thiourea (5k). Yield, 86%; mp: 185–187 °C; IR (KBr) $\nu_{\max}/\text{cm}^{-1}$ 3315, 3273, 2926, 1506. ¹H NMR δ 12.42 (s, 1H, NH, D₂O exchangeable), 10.59 (s, 1H, NH, D₂O exchangeable), 7.78 (d, *J* = 8.0 Hz, 2H, Ar-H), 7.62–7.40 (m, 2H, Ar-H), 7.31 (d, *J* = 8.0 Hz, 2H, Ar-H), 7.11–7.09 (m, 2H, Ar-H), 3.83 (s, 2H, CH₂), 2.37 (s, 3H, CH₃), 2.27 (s, 3H, CH₃). ¹³C NMR δ 184.10, 166.77, 149.39, 140.67, 137.98, 131.79, 130.81, 129.90, 129.64, 129.26, 126.97, 126.79, 126.21, 122.06, 23.93, 21.42, 20.98. MS (*m/z*): 354 (M⁺), 355 (M⁺ + 1). Anal. Calcd. for C₁₈H₁₈N₄S₂ (354.49): C, 60.99; H, 5.12; N, 15.81. Found: C, 61.23; H, 5.21; N, 15.97.

4.1.1.12. 1-(4-methoxyphenyl)-3-(5-(*p*-tolyl)-6H-1,3,4-thiadiazin-2-yl)thiourea (5l). Yield, 84%; mp: 187–190 °C; IR (KBr) $\nu_{\max}/\text{cm}^{-1}$ 3319, 3248, 2924, 1525. ¹H NMR δ 12.36 (s, 1H, NH, D₂O exchangeable), 10.57 (s, 1H, NH, D₂O exchangeable), 7.77 (d, *J* = 8.0 Hz, 2H, Ar-H), 7.61 (s, 1H, Ar-H), 7.42 (d, *J* = 7.3 Hz, 1H, Ar-H), 7.31 (d, *J* = 8.0 Hz, 2H, Ar-H), 6.87 (d, *J* = 7.6 Hz, 2H, Ar-H), 3.83 (s, 2H, CH₂), 3.74 (s, 3H, OCH₃), 2.36 (s, 3H, CH₃). ¹³C NMR δ 183.79, 166.58, 149.36, 140.67, 133.75, 131.83, 129.89, 126.96, 125.09, 123.60, 114.06, 113.84, 55.69, 23.89, 21.41. MS (*m/z*): 370 (M⁺). Anal. Calcd. for C₁₈H₁₈N₄O₂S₂ (370.49): C, 58.35; H, 4.90; N, 15.12. Found: C, 58.46; H, 4.98; N, 15.40.

4.1.1.13. 1-(5-(4-methoxyphenyl)-6H-1,3,4-thiadiazin-2-yl)-3-phenylthiourea (5m). Yield, 85%; mp: 183–185 °C; IR (KBr) $\nu_{\max}/\text{cm}^{-1}$ 3293, 3246, 2907, 1522. ¹H NMR δ 12.45 (s, 1H, NH, D₂O exchangeable), 10.62 (s, 1H, NH, D₂O exchangeable), 7.85 (d, *J* = 8.8 Hz, 2H, Ar-H), 7.59 (s, 2H, Ar-H), 7.30 (t, *J* = 7.5 Hz, 2H, Ar-H), 7.06 (d, *J* = 8.9 Hz, 3H, Ar-H), 3.83 (s, 5H, CH₂, OCH₃). MS (*m/z*): 356 (M⁺), 357 (M⁺ + 1), 358 (M⁺ + 2). Anal. Calcd. for C₁₇H₁₆N₄O₂S₂ (356.46): C, 57.28; H, 4.52; N, 15.72. Found: C, 57.21; H, 4.50; N, 15.66.

4.1.1.14. 1-(4-chlorophenyl)-3-(5-(4-methoxyphenyl)-6H-1,3,4-thiadiazin-2-yl)thiourea (5n). Yield, 80%; mp: 182–184 °C; IR (KBr) $\nu_{\max}/\text{cm}^{-1}$ 3298, 3251, 2931, 1515. ¹H NMR δ 12.49 (s, 1H, NH, D₂O exchangeable), 10.69 (s, 1H, NH, D₂O exchangeable), 7.86 (d, *J* = 8.7 Hz, 2H, Ar-H), 7.67–7.48 (m, 2H, Ar-H), 7.34 (d, *J* = 7.9 Hz, 2H, Ar-H), 7.06 (d, *J* = 8.7 Hz, 2H, Ar-H), 3.83 (s, 5H, CH₂, OCH₃). ¹³C NMR δ 183.93, 166.24, 156.85, 156.09, 148.13, 147.82, 135.48, 133.65, 133.43, 129.35, 128.74, 125.10, 123.70, 114.07, 113.85, 55.69, 23.77. MS (*m/z*): 390 (M⁺). Anal. Calcd. for C₁₇H₁₅ClN₄O₂S₂ (390.90): C, 52.23; H, 3.87; N, 14.33. Found: C, 52.47; H, 3.76; N, 14.58.

4.1.1.15. 1-(5-(4-methoxyphenyl)-6H-1,3,4-thiadiazin-2-yl)-3-(*p*-tolyl)thiourea (5o). Yield, 83%; mp: 176–178 °C; IR (KBr) $\nu_{\max}/\text{cm}^{-1}$ 3300, 3253, 2914, 1506. ¹H NMR δ 12.38 (s, 1H, NH, D₂O exchangeable), 10.57 (s, 1H, NH, D₂O exchangeable), 7.85 (d, *J* = 8.5 Hz, 2H, Ar-H), 7.61–7.31 (m, 2H, Ar-H), 7.26–7.04 (m, 4H, Ar-H), 3.83 (s, 5H, CH₂, OCH₃), 2.27 (s, 3H, CH₃). ¹³C NMR δ 183.96, 166.91, 161.48, 149.25, 137.99, 129.26, 128.71, 126.83, 123.19, 122.05, 114.72, 55.84, 23.97, 20.97. MS (*m/z*): 370 (M⁺), 371 (M⁺ + 1), 372 (M⁺ + 2). Anal. Calcd. for C₁₈H₁₈N₄O₂S₂ (370.49): C, 58.35; H, 4.90; N, 15.12. Found: C, 58.72; H, 4.82; N, 14.93.

4.1.1.16. 1-(4-methoxyphenyl)-3-(5-(4-methoxyphenyl)-6H-1,3,4-thiadiazin-2-yl)thiourea (5p). Yield, 78%; mp: 171–173 °C; IR (KBr)

$\nu_{\max}/\text{cm}^{-1}$ 3312, 3265, 2921, 1506. ¹H NMR δ 12.34 (s, 1H, NH, D₂O exchangeable), 10.54 (s, 1H, NH, D₂O exchangeable), 7.84 (d, *J* = 8.6 Hz, 2H, Ar-H), 7.60–7.41 (m, 2H, Ar-H), 7.05 (d, *J* = 8.6 Hz, 2H, Ar-H), 6.96–6.87 (m, 2H, Ar-H), 3.83 (s, 5H, CH₂, OCH₃), 3.74 (s, 3H, OCH₃). ¹³C NMR δ 183.70, 166.73, 155.95, 149.22, 133.79, 129.09, 128.70, 126.83, 125.08, 123.57, 114.84, 114.71, 114.04, 55.85, 55.69, 23.92. MS (*m/z*): 386 (M⁺), 387 (M⁺ + 1). Anal. Calcd. for C₁₈H₁₈N₄O₂S₂ (386.49): C, 55.94; H, 4.69; N, 14.50. Found: C, 55.74; H, 4.74; N, 14.43.

4.2. Biological evaluation

Biological evaluation was performed in the laboratory of the Egyptian company for the production of vaccines, sera and drugs (VACSERA, Giza, Egypt).

4.2.1. MTT cell viability assay

A549 or WI-38 cells were originally provided by American Type Culture Collection (ATCC, Manassas, VA, USA). The cells were rinsed with 0.25% (w/v) trypsin, 0.53 mM EDTA solution and Ca²⁺/Mg²⁺ free PBS (pH 7.2). Dulbecco's Modified Eagle's Medium (DMEM) supplemented with 10% FBS, 10 μg/ml of insulin and 1% penicillin/streptomycin was used for the cell culture. After that they were plated (100 μl/well) in 96-well cell culture plate overnight at 37 °C with 5% CO₂ and 95% humidity. 100 μl of serial 10-fold diluted sterile tested compounds were added to final concentrations of 0.01–100 μM and cultures were incubated for 24 h. The cell viability was identified using MTT assay kit (Sigma-aldrich, Saint Louis, Missouri, USA). Supernatants were wasted, 50 μl/well of (3-[4,5-dimethylthiazol-2-yl]-2,5-diphenyl tetrazolium bromide) (MTT) solution (5 mg/ml) was added and incubated at 37 °C with 5% CO₂ for 4 h. To dissolve the dark blue crystals, 100 μl of 0.04 N HCl in isopropanol was added to every well and mixed thoroughly. The absorbance was measured on Robonik P2000 spectrophotometer at a wave length of 490 nm using DMEM as a blank control. Results from three separate experiments were recorded and the viable cells percentage was calculated [26].

4.2.2. VEGFR2 kinase activity assay

VEGFR2 kinase activity was evaluated by means of VEGFR2 (KDR) Kinase Assay Kit (San Diego, CA, USA) according to manufacturer's instructions. In short, master mix (5X kinase buffer, 500 μM ATP, 50X PTK substrate and water) and compounds **5d**, **5i** and **5j** were added to corresponding wells. The reaction was initiated by adding VEGFR2 (positive control) to their designated wells. The plates were incubated at 30 °C for 45 min. After that, Kinase-Glo[®] MAX (Promega) was added to the reaction mixture as a detection reagent and the reaction was incubated again for 15 min at room temperature after which luminescence was measured using TECAN spark microplate reader. The concentration of the test solutions which inhibited the activity of the enzyme by 50% was determined.

4.2.3. B-RAF kinase activity assay

The inhibitory effects of **5d**, **5i** and **5j** on B-RAF (V600E) kinase activity were evaluated by means of B-RAF V600E Kinase Assay Kit (San Diego, CA, USA) according to manufacturer's instructions. In short, master mix (5X kinase buffer, 500 μM ATP, 5X B-RAF substrate, and water) and the compounds were added to corresponding wells. The reaction was initiated by adding B-RAF (V600E) or B-RAF WT (positive control) to their designated wells. The plates were incubated at 30 °C for 45 min. After that, Kinase-Glo[®] MAX (Promega) was added to the reaction mixture as a detection reagent and the reaction was incubated again for 15 min at room temperature after which luminescence was measured using TECAN spark microplate reader. The concentration of the test solutions which inhibited the activity of the enzyme by 50% was determined.

4.2.4. MMP9 inhibition screening assay

The inhibitory effects of **5d**, **5i** and **5j** on MMP9 were assayed using MMP9 Inhibitor Screening Assay Kit ab139448 (Abcam, UK) according to manufacturer's instructions. Briefly, MMP chromogenic substrate (25 mM Ac-PLG-[2-mercapto-4-methyl-pentanoyl]-LG-OC2H5), inhibitor (1.3 mM NNGH in DMSO), and human recombinant enzyme (2.68 U/ μ L) were diluted and brought to reaction temperature (37 °C). Then, colorimetric assay buffer was added to appropriate wells followed by MMP enzyme, MMP inhibitor and compounds **5d**, **5i** and **5j** were incubated for 60 min at 37 °C. The reaction was initiated by adding MMP substrate to each well and the colour intensity was measured at 412 nm using Robonik p2000 EIA reader. The concentration of the compounds which inhibited the activity of the enzyme by 50% was determined and compared to that of sorafenib.

4.2.5. DNA-flow cytometry analysis

A549 cells at a density of 1×10^6 cells were subjected to 0.32 μ M of compound **5j** or to 0.002% DMSO as a control for 24 h. The cells were separated by trypsinization, rinsed in ice-cold PBS and fixed in ice cold 70% ethanol. They were preserved in ethanol at 4 °C for at least 2 h then harvested by centrifugation. Subsequently, cells were washed in PBS and stained through Cycle TEST™ plus DNA Reagent Kit (ab139418 Propidium Iodide Flow Cytometry Kit) (Becton Dickinson Biosciences, San Jose, CA, USA). Cell cycle distribution was detected by a FACSCalibur flow cytometer (Becton Dickinson Biosciences, San Jose, CA, USA) and analyzed by Cell Quest software (Becton Dickinson) [41].

4.2.6. Annexin V-FITC apoptosis assay

Apoptotic cells were inspected by the Annexin V-FITC Apoptosis Detection Kit (Becton Dickinson Biosciences, USA). A549 cells were cultured and incubated for 24 h in the presence of 0.32 μ M of compound **5j** or 0.002% DMSO as a control. Cells were collected, rinsed and centrifuged. Thereafter, they were stained with a mixture of fluorescein isothiocyanate (FITC), Annexin V and propidium iodide and the reaction was left to proceed at room temperature for 30 min then analyzed using flow cytometry on FACSCalibur (Becton Dickinson Biosciences, San Jose, CA, USA). Quadrant analysis of co-ordinate dot plots was achieved using Cell Quest software. Unstained cells were used to adjust the photomultiplier voltage and for compensation setting adjustment in order to eliminate spectral overlap between the FL1 and FL2 signals [42].

4.2.7. Cell invasion and migration assays

Compound **5j** was assessed for its inhibitory effect on cell invasion and migration using two different methods namely: Trans well membrane assay and Wound healing assay as described before [43].

4.3. Docking study

A docking study was done using Molecular Operating Environment (MOE version 2008.10) [44]. So, the crystal structure of VEGFR2 (PDB ID code 4Asd) [45], B-RAF (PDB ID code 5HI2) [46] complexed with the sorafenib and MMP9 complexed with reverse hydroximate inhibitor (PDB ID code 1GKC) [47] were downloaded from Protein Data Bank <https://www.rcsb.org/pdb>. The standard protocol employed in MOE 2008.10 was used to perform the docking and the MOE's Pose Viewer utility was used for studying the geometry of the resulting complexes. The enzymes were prepared for docking in this manner: (1) The water molecules and co-crystallized ligand were removed. (2) 3D protonation for the enzyme, where hydrogen atoms were added at their standard geometry, the partial charges were computed, and the system was adjusted. Flexible ligand-rigid receptor docking of the most stable conformers was carried out by MOE-DOCK as follow: (1) Defining the receptor atoms as **Receptor + Solvent**. (2) Site of placement was defined as **Ligand Atoms**. (3) **Ligand atoms** were browsed from the conformational database of the least energetic conformers of the target

compounds. (4) Placement method was adjusted to **triangle matcher** in case of VEGFR2 and MMP9 while in case of B-RAF, the placement method was adjusted to **pharmacophore** generated based on the interaction of sorafenib with Glu501 and Asp594.5). The obtained poses were ranked using London dG as the scoring function and were exposed to ForceField refinement using the same scoring function. (6) Finally, the best scoring poses of the docked compounds were recognized and examined for protein-ligand interactions of the complexes.

Declaration of Competing Interest

The authors have declared no conflict of interest

Appendix A. Supplementary material

Supplementary data to this article can be found online at <https://doi.org/10.1016/j.bioorg.2019.103323>.

References

- [1] F. Bray, J. Ferlay, I. Soerjomataram, R.L. Siegel, L.A. Torre, A. Jemal, Global cancer statistics GLOBOCAN estimates of incidence and mortality worldwide for 36 cancers in 185 countries, *CA Cancer J. Clin.* 2018 (2018) 394–424.
- [2] K. Inamura, Lung cancer: understanding its molecular pathology and the 2015 WHO classification, *Front. Oncol.* 7 (2017) 193.
- [3] P. Maione, C. Gridelli, T. Troiani, F. Ciardiello, Combining targeted therapies and drugs with multiple targets in the treatment of NSCLC, *Oncologist* 11 (3) (2006) 274–284.
- [4] Y. Oguro, D.R. Cary, N. Miyamoto, M. Tawada, H. Iwata, H. Miki, A. Hori, S. Imamura, Design, synthesis, and evaluation of novel VEGFR2 kinase inhibitors: discovery of [1,2,4] triazolo [1,5-a] pyridine derivatives with slow dissociation kinetics, *Biorg. Med. Chem.* 21 (15) (2013) 4714–4729.
- [5] N. Ferrara, Vascular endothelial growth factor: basic science and clinical progress, *Endocr. Rev.* 25 (4) (2004) 581–611.
- [6] N. Ferrara, K.J. Hillan, W. Novotny, Bevacizumab (Avastin), a humanized anti-VEGF monoclonal antibody for cancer therapy, *Biochem. Biophys. Res. Commun.* 333 (2) (2005) 328–335.
- [7] K.J. Gotink, H.M. Verheul, Anti-angiogenic tyrosine kinase inhibitors: what is their mechanism of action? *Angiogenesis* 13 (1) (2010) 1–14.
- [8] L. Fu, L. Guo, Y. Zheng, Z. Zhu, M. Zhang, X. Zhao, H. Cui, Synergistic antitumor activity of low-dose c-Met tyrosine kinase inhibitor and sorafenib on human non-small cell lung cancer cells, *Oncol. Lett.* 15 (4) (2018) 5081–5086.
- [9] S. Sun, J. Zhang, N. Wang, X. Kong, F. Fu, H. Wang, J. Yao, Design and discovery of quinazoline- and thiourea-containing sorafenib analogs as EGFR and VEGFR-2 dual TK inhibitors, *Molecules* 23 (1) (2017) 24.
- [10] J. Yao, J. Chen, Z. He, W. Sun, W. Xu, Design, synthesis and biological activities of thiourea containing sorafenib analogs as antitumor agents, *Biorg. Med. Chem.* 20 (9) (2012) 2923–2929.
- [11] J. Yao, Z. He, J. Chen, W. Sun, H. Fang, W. Xu, Design, synthesis and biological activities of sorafenib derivatives as antitumor agents, *Bioorg. Med. Chem. Lett.* 22 (21) (2012) 6549–6553.
- [12] J. Yao, J. Chen, Z. He, W. Sun, H. Fang, W. Xu, Thiourea and thioether derivatives of sorafenib: synthesis, crystal structure, and antiproliferative activity, *Med. Chem. Res.* 22 (8) (2013) 3959–3968.
- [13] X. Kong, Z. Yao, Z. He, W. Xu, J. Yao, Design, synthesis and biological evaluation of thiourea and nicotinamide-containing sorafenib analogs as antitumor agents, *MedChemComm* 6 (5) (2015) 867–870.
- [14] S. Manjula, N.M. Noolvi, K.V. Parihar, S.M. Reddy, V. Ramani, A.K. Gadad, G. Singh, N.G. Kuttly, C.M. Rao, Synthesis and antitumor activity of optically active thiourea and their 2-aminobenzothiazole derivatives: a novel class of anticancer agents, *Eur. J. Med. Chem.* 44 (7) (2009) 2923–2929.
- [15] S. Saeed, N. Rashid, P.G. Jones, M. Ali, R. Hussain, Synthesis, characterization and biological evaluation of some thiourea derivatives bearing benzothiazole moiety as potential antimicrobial and anticancer agents, *Eur. J. Med. Chem.* 45 (4) (2010) 1323–1331.
- [16] P.-C. Lv, H.-Q. Li, J. Sun, Y. Zhou, H.-L. Zhu, Synthesis and biological evaluation of pyrazole derivatives containing thiourea skeleton as anticancer agents, *Biorg. Med. Chem.* 18 (13) (2010) 4606–4614.
- [17] S. Madabhushi, K.K.R. Mallu, V.S. Vangipuram, S. Kurva, Y. Poornachandra, C.G. Kumar, Synthesis of novel benzimidazole functionalized chiral thioureas and evaluation of their antibacterial and anticancer activities, *Bioorg. Med. Chem. Lett.* 24 (20) (2014) 4822–4825.
- [18] L.-Y. Ma, Y.-C. Zheng, S.-Q. Wang, B. Wang, Z.-R. Wang, L.-P. Pang, M. Zhang, J.-W. Wang, L. Ding, J. Li, Design, synthesis, and structure-activity relationship of novel LSD1 inhibitors based on pyrimidine-thiourea hybrids as potent, orally active antitumor agents, *J. Med. Chem.* 58 (4) (2015) 1705–1716.
- [19] D.E.A. Rahman, K.O. Mohamed, Synthesis of novel 1,3,4-thiadiazole analogues with expected anticancer activity, *D. Pharm. Chem.* 6 (1) (2014) 323–335.
- [20] J. Schröder, A. Henke, H. Wenzel, H. Brandstetter, H.G. Stammer, A. Stammer, W.D. Pfeiffer, H. Tschesche, Structure-based design and synthesis of potent matrix

- metalloproteinase inhibitors derived from a 6 H-1, 3, 4-thiadiazine scaffold, *J. Med. Chem.* 44 (20) (2001) 3231–3243.
- [21] B.S. Holla, B.K. Sarojini, B.S. Rao, P.M. Akberali, N.S. Kumari, V. Shetty, Synthesis of some halogen-containing 1,2,4-triazolo-1,3,4-thiadiazines and their antibacterial and anticancer screening studies—part I, *Il Farmaco* 56 (8) (2001) 565–570.
- [22] T.M. Abdel-Rahman, Synthesis, reactions, and anticancer activity of some 1,3,4-thiadiazole/thiadiazine derivatives of carbazole, phosphorus, Sulfur Silicon Relat. Elem. 181 (8) (2006) 1737–1754.
- [23] I.M. El-Deen, L. Barakat, M. Hisham, In vitro antitumor studies of some nitrogen heterocycles, *LJIR* 3 (7) (2017) 413–418.
- [24] G. Cox, J.L. Jones, K.J. O'Byrne, Matrix metalloproteinase 9 and the epidermal growth factor signal pathway in operable non-small cell lung cancer, *Clin. Cancer Res.* 6 (6) (2000) 2349–2355.
- [25] A. Novikova, N. Perova, L. Egorova, E. Bragina, Synthesis and properties of 1,3,4-thiadiazine derivatives. 1. Investigation of the condensation of substituted phenacyl bromides and bromoacetylpyridines with thiosemicarbazide, *Chem. Heterocycl. Compd.* 27 (6) (1991) 666–668.
- [26] T. Mosmann, Rapid colorimetric assay for cellular growth and survival: application to proliferation and cytotoxicity assays, *J. Immunol. Methods* 65 (1–2) (1983) 55–63.
- [27] H. Lavoie, M. Therrien, Regulation of RAF protein kinases in ERK signalling, *Nat. Rev. Mol. Cell Biol.* 16 (5) (2015) 281–298.
- [28] A.S. Dhillon, S. Hagan, O. Rath, W. Kolch, MAP kinase signalling pathways in cancer, *Oncogene* 26 (22) (2007) 3279–3290.
- [29] P.J. Roberts, C.J. Der, Targeting the Raf-MEK-ERK mitogen-activated protein kinase cascade for the treatment of cancer, *Oncogene* 26 (22) (2007) 3291–3310.
- [30] H. Davies, G.R. Bignell, C. Cox, P. Stephens, S. Edkins, S. Clegg, J. Teague, H. Woffendin, M.J. Garnett, W. Bottomley, Mutations of the BRAF gene in human cancer, *Nature* 417 (6892) (2002) 949.
- [31] M. Holderfield, M.M. Deuker, F. McCormick, M. McMahon, Targeting RAF kinases for cancer therapy: BRAF-mutated melanoma and beyond, *Nat. Rev. Cancer* 14 (7) (2014) 455–467.
- [32] E.T. Kimura, M.N. Nikiforova, Z. Zhu, J.A. Knauf, Y.E. Nikiforov, J.A. Fagin, High prevalence of BRAF mutations in thyroid cancer: genetic evidence for constitutive activation of the RET/PTC-RAS-BRAF signaling pathway in papillary thyroid carcinoma, *Cancer Res.* 63 (7) (2003) 1454–1457.
- [33] C.G.A.R. Network, Comprehensive molecular profiling of lung adenocarcinoma, *Nature* 511(7511) (2014) pp. 543–550.
- [34] H. Nagase, R. Visse, G. Murphy, Structure and function of matrix metalloproteinases and TIMPs, *Cardiovasc. Res.* 69 (3) (2006) 562–573.
- [35] R. Visse, H. Nagase, Matrix metalloproteinases and tissue inhibitors of metalloproteinases: structure, function, and biochemistry, *Circul. Res.* 92 (8) (2003) 827–839.
- [36] S.C. Pritchard, M.C. Nicolson, C. Lloret, J.A. McKay, V.G. Ross, K.M. Kerr, G.I. Murray, H.L. McLeod, Expression of matrix metalloproteinases 1,2,9 and their tissue inhibitors in stage II non-small cell lung cancer: implications for MMP inhibition therapy, *Oncol. Rep.* 8 (2) (2001) 421–424.
- [37] W. Sienel, J. Hellers, A. Morresi-Hauf, R. Lichtinghagen, W. Mutschler, M. Jochum, C. Klein, B. Passlick, K. Pantel, Prognostic impact of matrix metalloproteinase-9 in operable non-small cell lung cancer, *Int. J. Cancer* 103 (5) (2003) 647–651.
- [38] I. Pravst, M. Zupan, S. Stavber, Directed regioselectivity of bromination of ketones with NBS: solvent-free conditions versus water, *Tetrahedron Lett.* 47 (27) (2006) 4707–4710.
- [39] I. Pravst, M. Zupan, S. Stavber, Halogenation of ketones with N-halosuccinimides under solvent-free reaction conditions, *Tetrahedron* 64 (22) (2008) 5191–5199.
- [40] S.-J. Zhang, Z.-G. Le, A simple and selective procedure for α -bromination of alkanones with [Bmim] Br3 as a promoter under solvent-free conditions, *Chin. Chem. Lett.* 16 (12) (2005) 1590–1592.
- [41] A. Krishan, Rapid flow cytofluorometric analysis of mammalian cell cycle by propidium iodide staining, *J. Cell Biol.* 66 (1) (1975) 188–193.
- [42] D. Tao, J. Wu, Y. Feng, J. Qin, J. Hu, J. Gong, New method for the analysis of cell cycle-specific apoptosis, *Cytometry A* 57 (2) (2004) 70–74.
- [43] J. Pijuán, C. Barceló, D.F. Moreno, O. Maiques, P. Sisó, R.M. Martí, A. Macià, A. Panosa, In vitro cell migration, invasion, and adhesion assays: from cell imaging to data analysis, *Front. Cell. Dev. Biol.* 14 (7) (2019) 107.
- [44] Z.A. Kaplancikli, M.D. Altintop, G. Turan-Zitouni, A. Ozdemir, R. Ozic, G. Akalin, Synthesis, antimicrobial activity and cytotoxicity of novel oxadiazole derivatives, *J. Enzyme Inhib. Med. Chem.* 27 (1) (2012) 51–57.
- [45] M. McTigue, B.W. Murray, J.H. Chen, Y.-L. Deng, J. Solowiej, R.S. Kania, Molecular conformations, interactions, and properties associated with drug efficiency and clinical performance among VEGFR TK inhibitors, *Proc. Natl. Acad. Sci. USA* 109 (45) (2012) 18281–18289.
- [46] S.A. Foster, D.M. Whalen, A. Özen, M.J. Wongchenko, J. Yin, I. Yen, G. Schaefer, J.D. Mayfield, J. Chmielecki, P.J. Stephens, Activation mechanism of oncogenic deletion mutations in BRAF, EGFR, and HER2, *Cancer Cell* 29 (4) (2016) 477–493.
- [47] S. Rowsell, P. Hawtin, C.A. Minshull, H. Jepson, S.M. Brockbank, D.G. Barratt, A.M. Slater, W.L. McPheat, D. Waterson, A.M. Henney, Crystal structure of human MMP9 in complex with a reverse hydroxamate inhibitor, *J. Mol. Biol.* 319 (1) (2002) 173–181.